

Tetra-n-butylammonium Bromide (TBAB) Modified Cameroonian Local Clay Material for Adsorption of Crystal Violet Dye from Aqueous Solution

Constant Tcheka^{1*}, Raluca Pleșa Chicinaș², Andrada Măicăneanu³, Patrick Nkuigue Fotsing⁴, Hamou Moussout⁵, Richard Domga⁶

¹ Department of Chemistry, Faculty of Science, University of Ngaoundere, Ngaoundere, Cameroon

² Department of Chemical Engineering, Babeș-Bolyai University, Cluj-Napoca, Romania

³ Department of Chemistry, Indiana University of Pennsylvania, Indiana, Pennsylvania, USA

⁴ Department of inorganic Chemistry, Faculty of Science, University of Yaoundé I, Yaoundé, Cameroon

⁵ Laboratory of Chemistry/Biology Applied to the Environment, Faculty of Sciences, Moulay Ismaïl University, Meknes, Morocco

⁶ Department of Applied Chemistry, Ensai, University of Ngaoundéré, Ngaoundere, Cameroon

Email Address

cotchek@gmail.com (Constant Tcheka)

*Correspondence: cotchek@gmail.com

Received: 22 December 2017; **Accepted:** 10 January 2018; **Published:** 2 February 2018

Abstract:

The present paper reports the preparation and characterization of tetra-n-butylammonium bromide modified local clay material (TBAB-Clay) and its application as potential adsorbent material for Crystal Violet dye removal from aqueous solution. Major mineral phases, identified by X-ray powder diffraction (XRD), were illite and kaolinite, in addition to quartz and calcite as impurities. Characterization of the material was supplemented by scanning electron microscopy (SEM) and Fourier transform infrared (FTIR) spectroscopy. The kinetics of the adsorption process was studied using two models: pseudo-first-order and pseudo-second-order. Experimental data were best fitted with pseudo-second-order model. Three isotherm models namely Langmuir, Freundlich, and Dubinin-Radushkevich (D-R) were used to describe the adsorption process. The inclusion of non-linear regression analysis suggested the Langmuir model best described the adsorption process. The Langmuir isotherm predicted the maximum monolayer adsorption capacity of 115.54 mg g⁻¹ while the D-R isotherm suggested a physisorption process with a free energy value of 0.708 kJ mol⁻¹. Based on the obtained results it can be concluded that this modified clay material is a promising adsorbent for the removal of Crystal Violet dye from aqueous solution.

Keywords:

Clay Minerals, Illite, Kaolinite, TBAB-Clay, Crystal Violet Dye, Adsorption Equilibrium, Kinetic Studies

1. Introduction

Our environment (biomass and subsoil) includes a diversity of materials with useful characteristics for sustainable development so as to avoid compromising the possibilities of proper live as possible for future generations. The clay materials belong to these natural resources. Furthermore, water is very important and essential liquid for human and industrial activities. Many times, surface water contains several polluting substances, namely organic and inorganic. These substances coming from human and industrial activities (textile, leather, paper...) expose environment to toxic substances which disrupt all kind of land and aquatic life. Among the polluting substances, dyes are observable even at low concentrations in water [1,2]. Crystal Violet is a cationic dye with several industrial uses. Dyes are harmful for human health: once ingested, they can cause cancer, disrupt immune system and chromosomal chain and also induce respiratory disorders [3]. On the other hand, dyes present in waste water can adversely affect aquatic flora and fauna by reducing light solar radiation diffusion and photosynthesis, being hazardous and toxic to aquatic life [2,4–6]. The diversity and distinctness of hydric pollutants make the mechanism of their removal very complex. The elaboration and characterization of materials with various properties constitute required steps in the process of contaminated water treatment. As reported in many reviews, conventional methods for treating dye waste water, e.g. coagulation/flocculation, chemical oxidation, activated sludge process, are difficult, ineffective or present economic disadvantages [4]. Adsorption is a simple method used for dyes elimination from aqueous solutions [7,8]. The efficiency of the adsorption process depends on the used adsorbents and their capacities and cost. Several porous materials have been used as adsorbents for water remediation, such as activated carbon, zeolite, fly ash, clay minerals, biosorbents, and certain metal oxides based composites [9-12]. Several scientific papers reported that the preparation and use of activated carbon entail high costs [5]. From an environmental point of view, it is also worth noting the high energy that is spent in the production of activated carbons. Biomass by-products of and certain vertisols are used, in raw or chemically modified form, as alternative low cost adsorbent materials for the treatment of water loaded with dyes [5,13–15]. Among the low cost materials, clay minerals were proposed as potential candidate because of their low cost, abundance in the nature, high adsorption properties, and the presence of the electric charges on their interlamellar surface for potential ion-exchange [11]. The ability of clay materials in removal of dyes such as Cristal Violet has been proved by several scientific works [14,16–18]. Miyah et al. have carried out the removal of Crystal Violet dye from aqueous solutions using pyrophyllite [19]. Montmorillonite efficiency has been proved in the simultaneous adsorption of Crystal_Violet, cetyltrimethylammonium, and 2-naphthol by Zhu et al. [20]. Other researchers reported the effect of kaolinite activation on the adsorption of methylene blue [21], performances of treated vermiculite on the adsorption of cationic dyes [22], and the adsorption of methylene blue by the composite attapulgite/bentonite [23]. The importance attached to the study of clays and their application in the area of water treatment can be justified by their hydrophobic and organophylic property which are very important in water treatment process. Many recent scientific works related to the wastewater purification by adsorption on these adsorbents carry information or data on the different methods of synthesis, characterization and application. This study is focused on the possible usage of a local Cameroonian clay material as adsorbent and the behavior of its modified form with tertabutylammonium bromide (TBAB) on the removal of Crystal

Violet (CV) cationic dye from aqueous solution. The parameters as initial concentration, adsorbent quantity, kinetic and equilibrium studies were considered. The valorization of this clay as low cost adsorbent and natural resource for water treatment is also expected.

2. Materials and Methods

2.1. Materials

The local clay material used in this study was extracted from vertisol soil sample collected at Boboyo, in the far north region of Cameroon. All the chemicals used were of analytical grade and procured from different suppliers as follows: Crystal Violet (CV, $C_{25}H_{30}N_3Cl$; MW 407.98) was purchased from PENTA-Switzerland, tetra-n-butylammonium bromide (TBAB, purity $\geq 99.0\%$), and $AgNO_3$ were purchased from SIGMA-ALDRICH Corporation. The molecular structures of CV and TBAB are illustrated in Figure 1. A stock CV solution of 1000 g L^{-1} was prepared by dissolving the required amount of dye in distilled water. The derived solutions of desired concentrations were obtained by dilution of the stock solution.

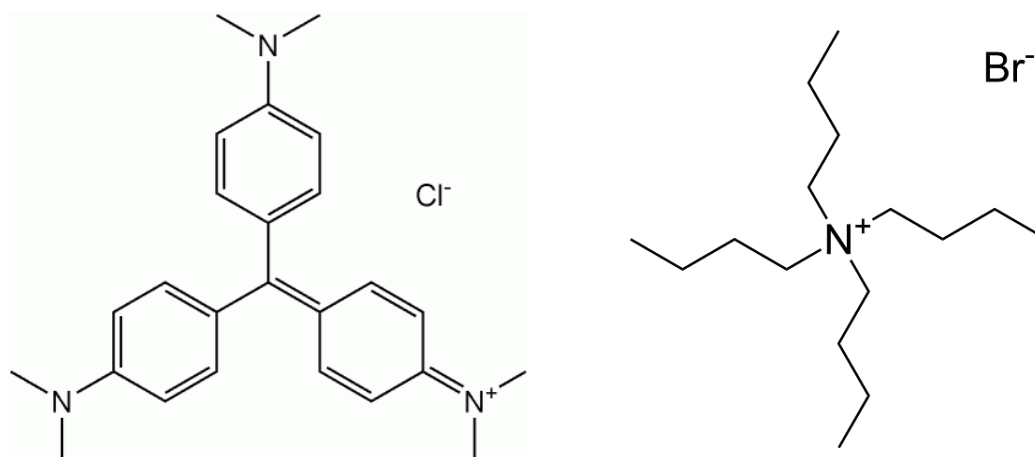


Figure 1. Molecular structures of (a) Crystal Violet dye and (b) TBAB

2.2. Preparation of organic modified clay (TBAB-Clay)

Firstly, the clay material has been washed with hydrogen peroxide in order to remove organic substances and other impurities, then washed with distilled water and dried in oven at $105\text{ }^{\circ}\text{C}$ for 24 hours. The clay fraction of the raw material has been obtained according to the following procedure: clay dispersion was placed in a graduated cylinder in order to allow particles $> 200\text{ }\mu\text{m}$ in size to settle down and the fine fraction, whose size was $< 200\text{ }\mu\text{m}$ was extracted at the time of the static sedimentation of the particles in suspension based on Stokes equation [24]:

$$t = 191.5 \times \frac{x}{d^2} \quad (1)$$

where: t is the necessary time (min), for a particle of diameter d (μm), to reach a depth of x (centimeter). The solid sample was then dried at $105\text{ }^{\circ}\text{C}$ for 24 h and sieved in order to collect particles sizes smaller than $200\text{ }\mu\text{m}$. The wet method described by Santos and Boaventura 2016, using the methylene blue adsorption was used in this work to assess the cation exchange capacity (CEC) of the Clay material [5]. This

parameter value was found to be 0.25 mmol g^{-1} . The purified clay (P-Clay) obtained as described above was converted into organoclay form by treatment with TBAB. For the synthesis, the amount of TBA⁺ ions corresponding to 100% of the cation exchange capacity of the purified Clay was added to a 1% slurry. The suspension was stirred at 400 rpm for 4 h at room temperature, filtered, washed several times with distilled water and then dried at 60°C for 24 h. The product obtained was powdered and sieved to get a particle size of $200 \mu\text{m}$. This product was referred to as TBAB-Clay.

2.3. Characterization of Adsorbent Materials

IR spectra of the sample was obtained using a FT/IR-4100 Spectrophotometer (JASCO Benelux BV) in KBr pellets. Scanning electron microscopy (SEM) images were obtained with TESCAN, VEGA II model equipment for Clay material. A semi-quantitative X-ray powder diffraction method was used to determine mineral composition. X-ray diffraction analyses on powders were performed using a Siemens Bruker D8 Advance unit with Co-K α anticathode ($\lambda = 1.7903 \text{ \AA}$). The diffractograms were recorded from 5° to 64° degrees with analytic conditions of 40 mA, 20 kV, 0.02° steps. d-spacing, d_{hkl} , corresponding to different diffraction pics have been calculated using Bragg's equation and JCPDS (Joint Committee on Powder Diffraction Standards) files were utilized in order to identify the crystalline compounds.

2.4. Adsorption Experiments

2.4.1. Analytical Methods

CV dye concentrations in aqueous solution were analyzed using a T70+ UV-VIS spectrophotometer with wavelength range of 190-1100 nm from PG Instruments Ltd, at the wavelengths of maximum absorbance, $\lambda_{\text{max}} = 591 \text{ nm}$. Calibration straight lines ($R^2 = 0.9995$) were obtained in $2.0\text{-}10.0 \text{ mg L}^{-1}$ range. Before analyses, all aqueous samples were centrifuged for 5 min at 5000 rpm (EBA 21 centrifuge).

2.4.2. Equilibrium Adsorption Studies

Batch experiments were carried out by mixing 0.1 g of adsorbent with 50.0 mL of known concentration of CV solution. The mixtures were maintained under magnetic stirring at 500 rpm for 6 h at 38°C , to ensure that the equilibrium was reached. Effect of adsorbent quantity, in $0.10\text{-}2.00 \text{ g}$ range using 50.0 mL of 200 mg L^{-1} dye solution was studied. Effect of contact time was studied on three initial dye concentrations of 200, 225, and 250 mg L^{-1} using sampling at predetermined time intervals (5 - 360 min). The effect of initial dye concentration ($10 - 250 \text{ mg L}^{-1}$) was also investigated at 28°C . All the experiments were conducted at the initial solution pH (7.3). Pseudo-first-order and pseudo-second-order models were used to give an insight into the adsorption kinetic mechanisms. The Langmuir, Freundlich, and Dubinin-Radushkevich isotherm models were used to describe the adsorption process. The amount of dye adsorbed per gram of adsorbent, (mg g^{-1}) and adsorption efficiency, (%) were calculated using the following equations:

$$q_{t(e)} = \frac{(C_i - C_{t(e)})V}{m} \quad (2)$$

$$\eta = \frac{(C_i - C_e)}{C_i} \times 100 \quad (3)$$

where C_i is the initial dye concentration (mg L^{-1}), C_e and C_t are the equilibrium and time t dye concentrations respectively (mg L^{-1}), V is the volume of CV solution (L), and m is the adsorbent quantity (g).

3. Results and Discussion

3.1. Adsorbents Characterization

3.1.1. XRD Analysis

The mineralogical composition of the purified local Clay (P-Clay) sample was determined from the X-ray diffraction pattern (Figure 2). Illite mineral has been identified by the pics with d-spacing values of 10.05 Å, 3.51 Å and 3.20 Å, while the pics at 7.25, 4.4 and 4.03 Å were ascribed to Kaolinite. The following mineral phases were identified: illite, kaolinite, quartz, and calcite. It can be observed that the intensity of the peaks attributed to crystalline minerals such as quartz decrease after modification of the clay with TBAB. From this observation, it can be concluded that after modification of the clay material, TBAB molecules cover the surface of the mineral phases and reduce peaks intensity.

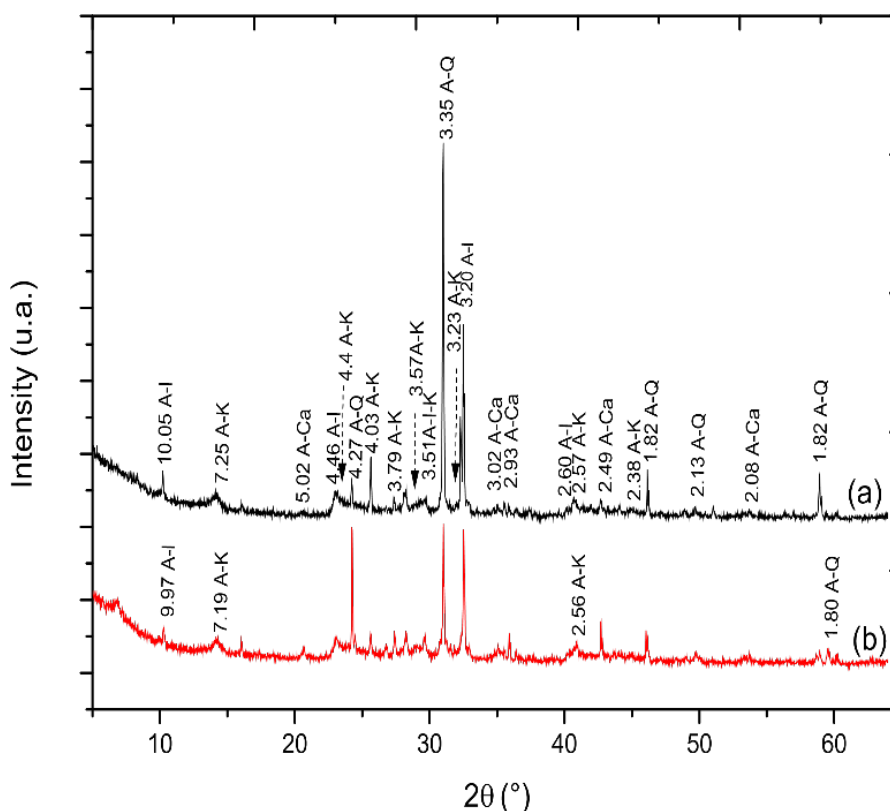


Figure 2. XRD patterns of P-Clay (a) and TBAB-Clay (b) (I: Illite, K: Kaolinite, Ca: Calcite, Q: Quartz)

3.1.2. FTIR Analysis

The FTIR spectra of P-Clay and TBAB-Clay are shown in Figure 3. Various functional groups are observed. Adsorption bands at 3697 cm^{-1} can be ascribed to O – H stretching vibrations which originate from Al-OH and Si-OH [25]. The envelope at

3624 cm^{-1} belongs to OH stretching of H-bonded water, with a shoulder near 3445 cm^{-1} , due to the overtone of the bending vibration of H_2O observed at 1638 cm^{-1} [25]. Absorption band at 3445 cm^{-1} weakens and shifts to a lower wave number 3421 cm^{-1} for TBAB-Clay. The peaks at 1007 and 1033 cm^{-1} were assigned to characteristic bands of silicates which were mostly related to stretching vibrations of M-O (where M = Si, Al), and agreed well within the range $1103\text{--}1036\text{ cm}^{-1}$ [26], and $1200 - 600\text{ cm}^{-1}$ [27], while the bands at 536 and 466 cm^{-1} were due to Al-O-Si and Si-O-Si bending vibrations, respectively. The peak at 912 cm^{-1} was responsible for Al-Al-OH group deformation [25,27,28]. The band at 2965 cm^{-1} (TBAB-Clay) is attributed to the C-H stretching vibrations of the TBAB [17]. Compared with the IR spectra of P-Clay, the absorption band of -OH bending vibration of interlayer water P-Clay (1638 cm^{-1}) moved to 1631 cm^{-1} for TBAB-Clay. Simultaneously, the intensity of this absorption band decreases, which indicated the water content reduced with the replacement of the hydrated cations by TBA^+ . This observation showed that the surface properties of P-Clay had been changed from hydrophilic to hydrophobic by modifying it with TBAB [16].

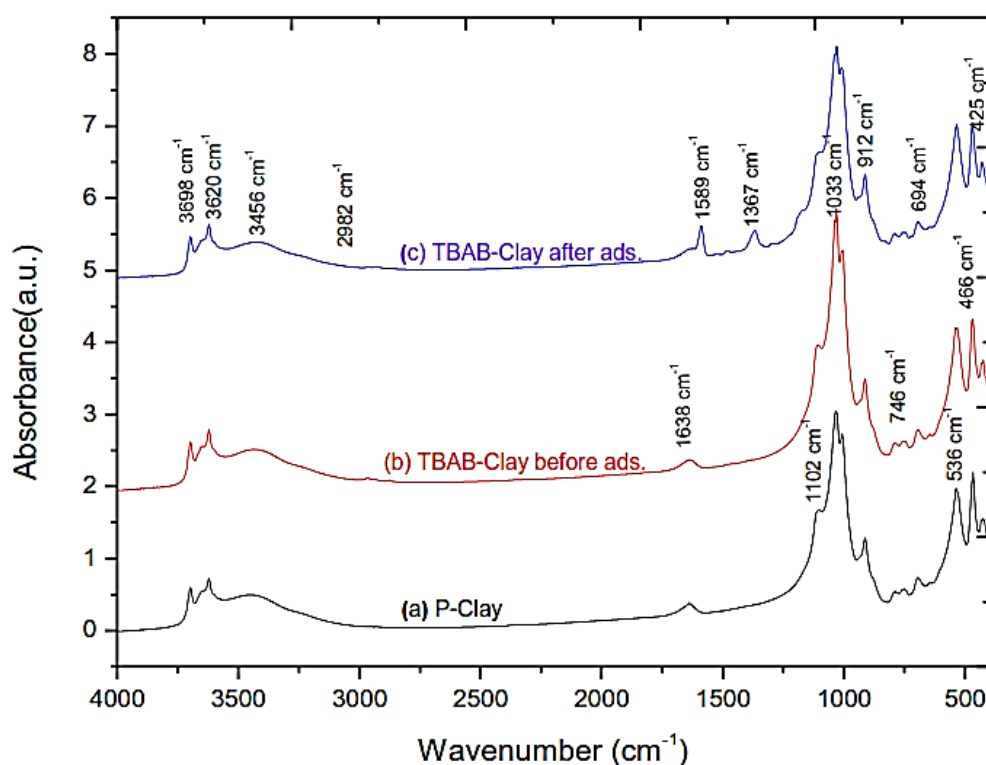


Figure 3. FTIR spectra of P-Clay and TBAB-Clay samples

3.1.2. Scanning Electron Microscopy

Typical SEM micrographs of P-Clay and TBAB-Clay are shown in Figure 4. It can be seen that the P-Clay shows small particles (Figure 4a), but after modification with TBAB, its form changed slightly and led to a large particles and coarse porous surface.

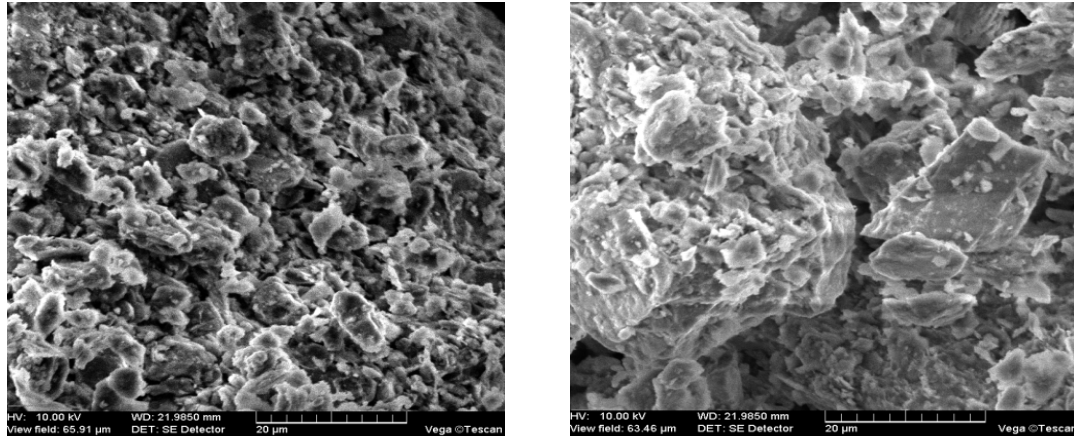


Figure 4. SEM images of P-Clay (a) and TBAB-Clay (b)

3.2. Crystal Violet Adsorption

3.2.1. Effect of Adsorbent Quantity

P- and TBAB-Clay quantity influence over the CV removal is presented in Figure 5. It can be seen that as the adsorbent quantity increases, adsorption capacity decreases. The obtained results show that modified clay (TBAB-Clay) is a better adsorbent than P-Clay. The optimum adsorbent quantity was found to be 100 mg for both adsorbents P-Clay and TBAB-Clay, with q_e values of 75.62 mg g^{-1} and 85.49 mg g^{-1} and percentage removal values of 95.56% and 98.44%, respectively. Adsorbent quantities higher than 100 mg displayed a gradual decrease in q_e , while there was a small increase in percentage removal when higher mass was used. The decrease in q_e at higher dosage is due to a decrease in the number of occupied sites per unit mass [6,29]. In terms of removal efficiencies an increase was observed (Figure 5b) if a higher quantity of adsorbent is added due to the fact that for the same initial concentration a higher surface (increased number of adsorption sites) will be available for adsorption [29].

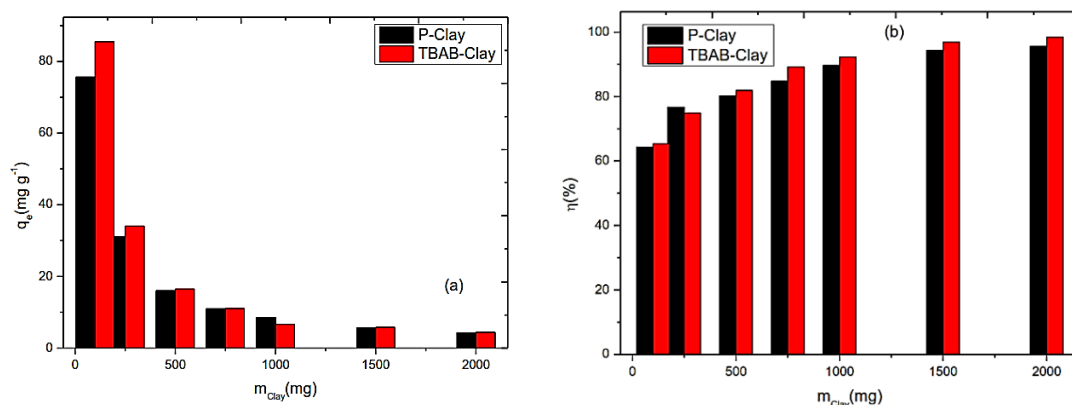


Figure 5. The effect of P-Clay and TBAB-Clay quantity on CV adsorption over the (a) adsorption capacity and (b) removal efficiency; Conditions: 50.0 mL, 200 mg L^{-1} , 7.3 pH, 28°C , 500 rpm

3.4. Effect of Contact Time and Kinetics Studies

The evaluation of the effect of contact time is essential because it provides fundamental information on how fast the adsorption process reaches equilibrium. From the results presented in Figure 6, it was observed the fast dye adsorption at initial stage, which became gradually slower as equilibrium was approached. The time required to reach equilibrium was found to be 240 min. Numerous and vacant active surface sites of adsorbent were available in the early stages of the adsorption, while as the contact time increased, the number of vacant sites decreased, thereby slowing down the adsorption process. Similarly, the increase of the initial dye concentration led to higher loading rates of the adsorbate molecule, which was attributed to the enhanced driving force of the concentration gradient to the vacant sites of adsorbent [29].

Adsorption is a complex process whereby it is influenced by several parameters related to adsorbent and to the physicochemical conditions under which the process is carried out [6]. In order to investigate the adsorption mechanism, the linear form of the pseudo-first-order [30] and the pseudo-second-order [31] kinetic rate equations were used, equations (3) and (4), respectively:

$$\log(q_e - q_t) = \log(q_e) - \frac{t}{2.303} k_1 \quad (4)$$

$$\frac{t}{q_t} = \frac{1}{k_2 q_e^2} + \frac{t}{q_e} \quad (5)$$

Where q_t and q_e represent the amount of dye adsorbed at equilibrium (mg g^{-1}) and at time t (min), and k_1 (min^{-1}) and k_2 ($\text{g mg}^{-1} \text{min}^{-1}$) are the pseudo-first-order and pseudo-second-order rate constants, respectively. The rate constants k_1 , k_2 , and the calculated q_e (cal) obtained from equations (4) and (5) along with the experimental q_e (exp) (Figure 6) and coefficients of determination R^2 , are presented in Tables 1 and 2.

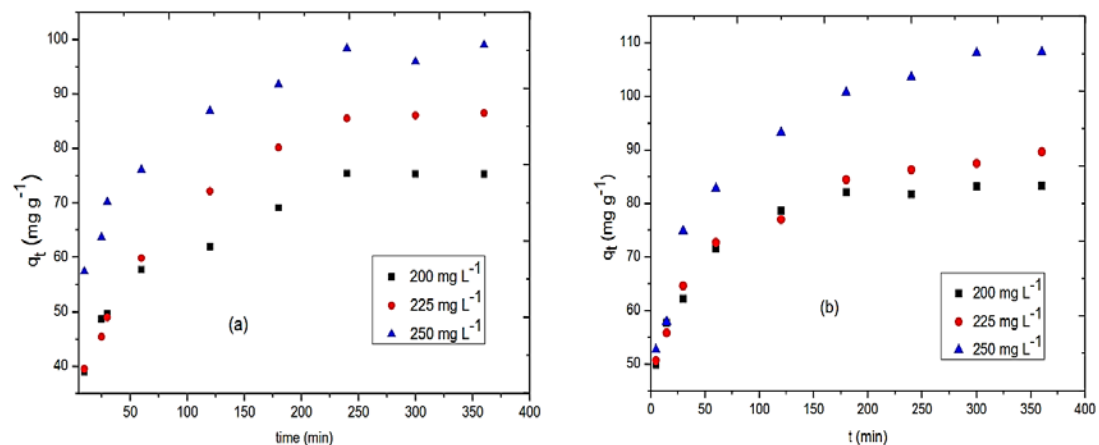


Figure 6. Effect of contact time and initial concentration of CV adsorption on P-Clay (a) and on TBAB-Clay (b). Conditions: CV concentration (■) 200, (●) 225 and (▲) 250 mg L^{-1} , 50.0 mL, 0.10 g, 7.3 pH, 28°C, 500 rpm

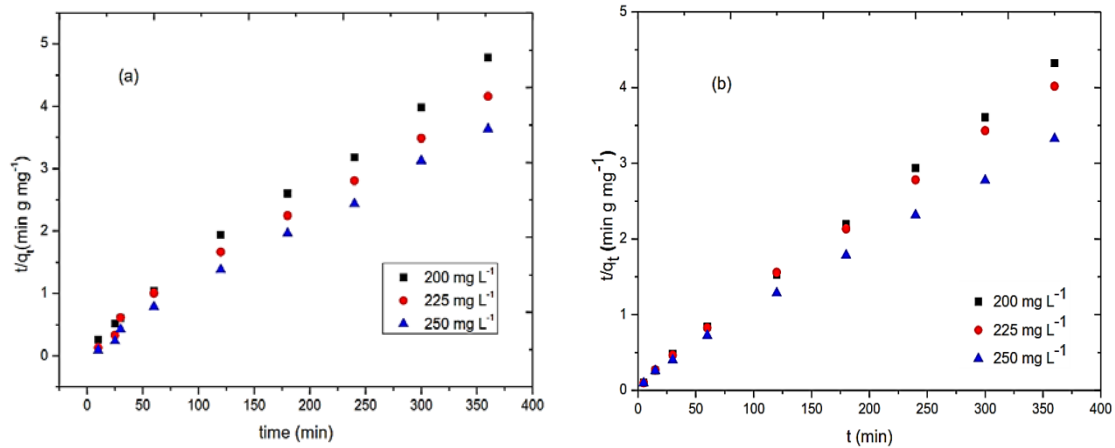


Figure 7. Pseudo-second-order kinetic modelling of CV adsorption on P-Clay (a) and TBAB-Clay (b). Conditions: CV concentration (■) 200, (●) 225 and (▲) 250 mg L^{-1} , 50.0 mL, 0.10 g, 7.3 pH, 28°C, 500 rpm

Table 1. Kinetic constants of the pseudo-first- and pseudo-second-order models for CV adsorption on P-Clay.

CV dye		Pseudo-first-order model			Pseudo-second-order model		
Conc. (mg L^{-1})	$q_e(\text{exp})$ (mg g^{-1})	k_1 (min^{-1})	$q_e(\text{cal})$ (mg g^{-1})	R^2	k_2 ($\text{g mg}^{-1}\text{min}^{-1}$)	$q_e(\text{cal})$ (mg g^{-1})	R^2
200	75.4	0.045	54.11	0.841	0.0007	79.36	0.997
225	86.5	0.043	79.52	0.943	0.0005	90.91	0.996
250	98.95	0.043	70.60	0.770	0.0008	101.01	0.998

Table 2. Kinetic constants of the pseudo-first- and pseudo-second-order models for CV adsorption on TBAB-Clay

CV dye		Pseudo-first-order model			Pseudo-second-order model		
Conc. (mg L^{-1})	$q_e(\text{exp})$ (mg g^{-1})	k_1 (min^{-1})	$q_e(\text{cal})$ (mg g^{-1})	R^2	k_2 ($\text{g mg}^{-1}\text{min}^{-1}$)	$q_e(\text{cal})$ (mg g^{-1})	R^2
200	83.26	0.041	37.77	0.966	0.0010	84.74	0.999
225	89.65	0.041	64.81	0.847	0.0009	90.91	0.998
250	108.27	0.041	131.55	0.812	0.0005	112.36	0.998

Based on the obtained R^2 values (Tables 1 and 2) and the fact that $q_e(\text{exp})$ are in better agreement with the $q_e(\text{cal})$ values when pseudo-second-order model was used to model the adsorption system, it can be concluded that the adsorption of CV by P-Clay and TBAB-Clay it is better described by this model. This behavior was explained by considering that adsorbate molecules may occupy two adsorption sites on the solid surface instead of only one [15,25,32,33].

3.5. Adsorption Isotherm

Adsorption isotherms are important for the description of how molecules of adsorbate interact with the adsorbent surface [34]. Three isotherm models Langmuir, [35], Freundlich, [36], and Dubinin-Radushkevich [37,38] were used to describe the adsorption process of CV onto both Clay adsorbents. Table 3 shows the non-linear and linear equations of each isotherm model.

Table 3. Non-linear and linearized isotherm model equations

Isotherm model	Non-linear equation	Linearized equation	Plot	Eqs.
Langmuir	$q_e = \frac{q_{\max} \cdot K_L \cdot C_e}{1 + K_L \cdot C_e}$	$\frac{C_e}{q_e} = \frac{1}{K_L \cdot q_{\max}} + \frac{C_e}{q_{\max}}$	$\frac{C_e}{q_e}$ vs. C_e	(6)
Freundlich	$q_e = K_F \cdot C_e^{1/n_F}$	$\ln q_e = \frac{1}{n_F} \ln C_e + \ln K_F$	$\ln q_e$ vs. $\ln C_e$	(7)
Dubinin-Radushkevich	$q_e = q_D \cdot e^{-k_{ad} \cdot \varepsilon^2}$	$\ln q_e = \ln q_D - k_{ad} \cdot \varepsilon^2$	$\ln q_e$ vs. ε^2	(8)

where q_{\max} is the maximum monolayer adsorption capacity of the adsorbent (mg g^{-1}), K_L is the Langmuir adsorption constant (L mg^{-1}) which is related to the free energy of adsorption, and C_e (mg L^{-1}) is the equilibrium dye concentration. K_F [$\text{mg g}^{-1}(\text{L mg}^{-1})^{1/n}$] is Freundlich constant an indicator of the adsorption capacity of the adsorbent while n_F indicates favorability of the adsorption process (adsorption intensity) or surface heterogeneity where n_F value between 1 and 10 represents favorable adsorption. q_D is the theoretical isotherm saturation capacity (mg g^{-1}), B_D ($\text{mol}^2 \text{J}^{-2}$) and ε are D-R isotherm constants. ε can be determined using equation (9).

$$\varepsilon = RT \ln \left(1 + \frac{1}{C_e} \right) \quad (9)$$

The mean free energy of adsorption (E , kJ mol^{-1}) can be calculated by using equation (10).

$$E = \frac{1}{\sqrt{2B_D}} \quad (10)$$

Langmuir adsorption isotherm describes quantitatively the formation of a monolayer adsorbate on the outer surface of the adsorbent, and after that no further adsorption takes place. Thereby, the Langmuir represents the equilibrium distribution of adsorbate (dye molecules) between the solid and liquid phases [39,40]. The model assumes uniform energies of adsorption onto the surface and no transmigration of adsorbate in the plane of the surface. The essential features of the Langmuir isotherm may be expressed in terms of equilibrium parameter R_L , which is a dimensionless constant referred to as separation factor or equilibrium parameter [40].

$$R_L = \frac{1}{(1 + K_L C_0)} \quad (11)$$

where C_0 is the highest initial dye concentration. R_L value indicates the adsorption nature to be either unfavorable ($R_L > 1$), linear ($R_L = 1$), favorable ($0 < R_L < 1$), and irreversible ($R_L = 0$) [6].

The Freundlich isotherm model takes account of multilayer coverage where adsorption is still possible on the adsorbate saturated adsorbent's surface. It is applicable for adsorption on heterogeneous surfaces with uniform energy distribution and reversible adsorption [39].

Dubinin–Radushkevich isotherm is usually employed to explain the mechanism of adsorption with respect to Gaussian energy distribution onto a heterogeneous surface and determine the nature of adsorption as physical or chemical based on the free mean sorption energy [41,42]. It was reported that chemical adsorption predominates if free mean energy value (E) was in the range of 8-16 kJ mol⁻¹ whereas E value lower than 8 kJ mol⁻¹ follows the physisorption process [41].

Table 4. Adsorption isotherm parameters for CV adsorption on P-Clay and TBAB-Clay.

Conditions: Concentration range: [10-250] mg L⁻¹, $m = 0,10$ mg, $t = 180$ min, $V = 0,05L$, $T = 28^{\circ}C$

Adsorbents	Langmuir			Freundlich			Dubinin-Radushkevich			
	q_m (mg g ⁻¹)	K_L (L mg ⁻¹)	R^2	K_F [mg g ⁻¹ (L mg ⁻¹) ^{1/n_F}]	n_F	R^2	q_D (mg g ⁻¹)	B_D (mol ² kJ ⁻²)	E (kJ mol ⁻¹)	R^2
TBAB-Clay	115.54	1.117	0.966	44.083	3.57	0.897	100.80	$1.000 \cdot 10^{-6}$	0.708	0.887
P-Clay	103.21	0.303	0.960	29.656	3.12	0.835	94.00	$1.160 \cdot 10^{-6}$	0.762	0.705

Isotherms model parameters are obtained by determining the slope and intercept or their linear plots as shown in Table 3. In order to choose the isotherm model that best describes the experimental data; three comparisons were made based on the R^2 , and the non-linear regression plot. Table 4 shows the isotherm parameters while Figure 8 shows the non-linear regression plots of the three isotherm models and experimental data.

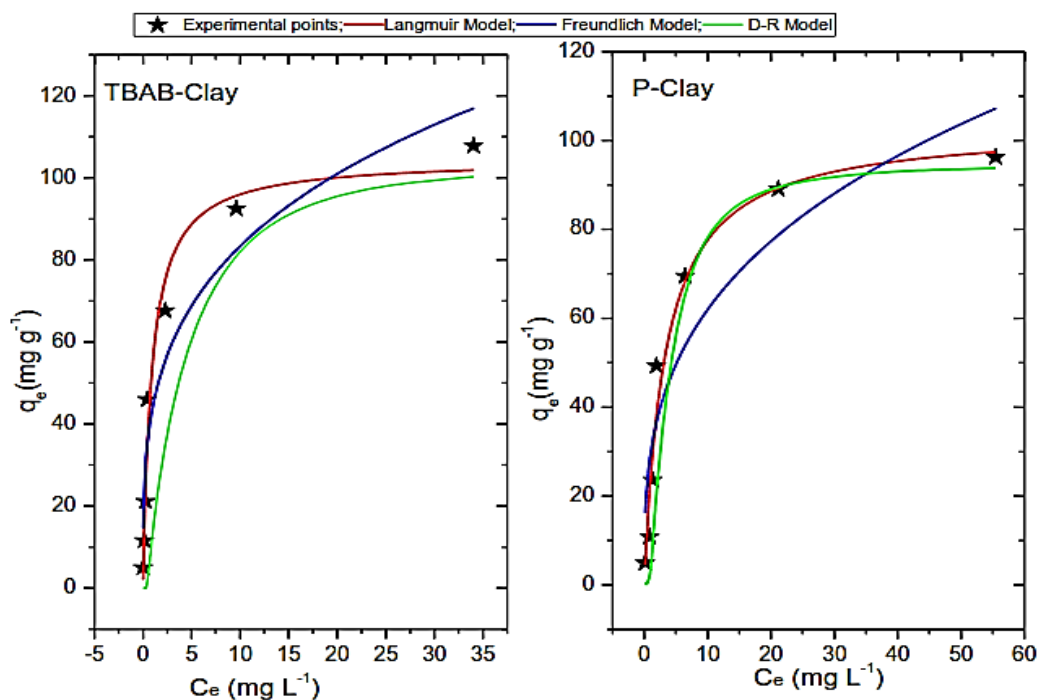


Figure 8. Non-linear isotherm modelling of CV adsorption on P-Clay and TBAB-Clay

Comparing the R^2 values, the Langmuir isotherm model has the highest value followed by the Freundlich, and Dubinin-Radushkevich for both adsorbents (P-Clay and TBAB-Clay), which indicates that Langmuir model was the best fit to the experimental data. When comparing the non-linear plot and experimental data in Figure 7, the Langmuir is again the closest to the experimental data. From these

comparisons, it can be concluded that the Langmuir model is the best fit to the experimental data. The values of n_F and R_L , indicate that the adsorption of CV on P- and TBAB-Clay is a favorable process. Low free energy value of 0.762 and 0.708 kJ mol⁻¹ obtained in this study indicates that CV adsorption by P- and TBAB-Clay takes place as physisorption [39,43]. q_m values corresponding to Langmuir monolayer capacity are close (103.21 And 115.54 mg g⁻¹ for P- and TBAB-Clay, respectively).

3.6. Comparison of Monolayer Adsorption of CV onto Various Adsorbents

The performance and the quality of an adsorbent material are appreciated based on q_{max} value. An adsorbent is of the best quality when it present a higher adsorption capacity at a low cost. A comparison of the adsorption capacities CV onto various adsorbents is shown in Table 5. The adsorption capacity of TBAB- clay is comparable with those of other adsorbents. The value obtained in this study (115.54 mg g⁻¹) shows that TBAB-Clay has a good affinity for CV dye molecules (Table 5).

Table 5. Comparison of the adsorption capacities of basic dyes from the literature on various adsorbents.

Adsorbent	q_{max} (mg g ⁻¹)	Ref.
CoFe ₂ O ₄ nanoparticles	105,04	[44]
Palygorskite	158,76	[45]
Tomato Plant Root	94,34	[46]
SDS coated MNPs	166,7	[42]
Magnesium oxide coated bentonite	496	[47]
HDTMA Bentonite	365,11	[48]
Nanoporous hypercrosslinked polyaniline	227	[49]
Modified Ball Clay	62.5	[15]
Sepiolite	110	[5]
p-MBIM-Bentonite	128.23	[50]
HDTMA-Clay	56.81	[14]
Walnut shell	90.8	[6]
Attapulgit/Bentonite	95.15	[23]
TBAB-Clay	114.54	This study

4. Conclusions

A local clay material and its modified form, were tested as adsorbent for Crystal Violet dye removal from aqueous solutions. The modified form, TBAB-Clay, was prepared by ion exchange method using tetra-*n*-butylammonium bromide salt and characterized by XRD, FTIR, and SEM. Illite, Kaolinite, Quartz, and Calcite were the mineral phases present in the clay material as revealed XRD pattern. Adsorption experiments showed that the removal of CV by this local clay material was possible even on the purified form and the kinetics could be described well by the pseudo-second-order model ($R^2 > 0.99$) with an equilibrium time of 4 h. Langmuir isotherm model best describes the adsorption process with maximum monolayer adsorption capacity of 115.54 mg g⁻¹ for TBAB-Clay. R_L and n_F values indicate that the adsorption of CV is favorable. Free energy value of 0.708 kJ mol⁻¹ calculated using Dubinin-Radushkevich isotherm indicates that the adsorption of CV onto TBAB-Clay takes place as physisorption. All these results suggested that this local clay, just

purified or modified with TBAB is a good candidate as low-cost adsorbent for the removal of CV from aqueous solution.

Conflicts of Interest

The authors declare that there is no conflict of interest regarding the publication of this article.

Acknowledgments

This work has been accomplished under the framework of Programme de Bourses Postdoctorales “Eugene Ionescu” 2016. The authors gratefully acknowledge Agence Universitaire de la Francophonie, Romania for their financial support.

References

- [1] Güzel F, Say H, Akkaya G, et al. Elimination of anionic dye by using nanoporous carbon prepared from an industrial biowaste. *J. Mol. Liq.* 2014; 194:130–140.
- [2] Ramesh KSBST. Removal of dyes using agricultural waste as low-cost adsorbents : a review. *Appl Water Sci.* 2013; 3:773–790.
- [3] Verma Y. Toxicity Evaluation of Effluents from Dye and Dye Intermediate Producing Industries Using Daphnia Bioassay. *Internet J. Toxicol.* 2007; 4:1–7.
- [4] Pengthamkeerati P, Satapanajaru T, Singchan O. Sorption of reactive dye from aqueous solution on biomass fly ash. *J. Hazard. Mater.* 2008; 153:1149–1156.
- [5] Santos SCR, Boaventura RAR. Adsorption of cationic and anionic azo dyes on sepiolite clay : Equilibrium and kinetic studies in batch mode. *J. Environ. Chem. Eng.* 2016; 4:1473–1483.
- [6] Dahri MK. Water remediation using low cost adsorbent walnut shell for removal of malachite green : Equilibrium, kinetics, thermodynamic and regeneration studies. *J. Environ. Chem. Eng.* 2014; 2:1434–1444.
- [7] Gupta VK. Application of low-cost adsorbents for dye removal – A review. *J. Environ. Manage.* 2009; 90:2313–2342.
- [8] Kooli F, Liu Y, Al-faze R, et al. Applied Clay Science Effect of acid activation of Saudi local clay mineral on removal properties of basic blue 41 from an aqueous solution. *Appl. Clay Sci.* 2015; 116–117:23–30. Available from: h.
- [9] Duta A, Visa M. Simultaneous removal of two industrial dyes by adsorption and photocatalysis on a fly-ash –TiO₂ composite. *Journal Photochem. Photobiol. A Chem.* 2015; 306:21–30.
- [10] Hussein FH, Halbus AF, Lafta AJ, et al. Preparation and Characterization of Activated Carbon from Iraqi Khestawy Date Palm. *J. Chem.* 2015; 1–8.
- [11] Rahman A, Urabe T, Kishimoto N. Color removal of reactive procion dyes by clay adsorbents. *Procedia Environ. Sci.* 2013; 17:270–278.
- [12] Saygılı Hasan GF. High surface area mesoporous activated carbon from tomato processing solid waste by zinc chloride activation : process optimization, characterization and dyes adsorption. *J. Clean. Prod.* 2016; 113:995–1004.

- [13] Visa M, Bogatu C, Duta A. Tungsten oxide – fly ash oxide composites in adsorption and photocatalysis. *J. Hazard. Mater.* 2015; 286:244–256. Available from: h.
- [14] Sofía Arellano-Cárdenas, Socorro López-Cortez, Maribel Cornejo-Mazón JCM-G, Departamento. Study of malachite green adsorption by organically modified clay using a batch method. *Appl. Surf. Sci.* 2013; 280:74–78.
- [15] Auta M, Hameed BH. Modified mesoporous clay adsorbent for adsorption isotherm and kinetics of methylene blue. *Chem. Eng. J.* 2012; 198–199:219–227.
- [16] Wang L, Wang A. Adsorption properties of Congo red from aqueous solution onto surfactant-modified montmorillonite. 2008; 160:173–180.
- [17] Xia C, Jing Y, Jia Y, et al. Adsorption properties of congo red from aqueous solution on modified hectorite: Kinetic and thermodynamic studies. *Desalination.* 2011; 265:81–87.
- [18] Chen D, Chen J, Luan X, et al. Characterization of anion – cationic surfactants modified montmorillonite and its application for the removal of methyl orange. *Chem. Eng. J.* 2011; 171:1150–1158. Available from: <http://dx.doi.org/10.1016/j.cej.2011.05.013>.
- [19] Miyah Y, Lahrichi A, Idrissi M. Assessment of adsorption kinetics for removal potential of Crystal Violet dye from aqueous solutions using Moroccan pyrophyllite. 2016;
- [20] Zhu R, Chen Q, Liu H, et al. Applied Clay Science Montmorillonite as a multifunctional adsorbent can simultaneously remove crystal violet, cetyltrimethylammonium, and 2-naphthol from water. *Appl. Clay Sci.* [Internet]. 2014; 88–89:33–38. Available from: <http://dx.doi.org/10.1016/j.clay.2013.12.010>.
- [21] Gao W, Zhao S, Wu H, et al. Applied Clay Science Direct acid activation of kaolinite and its effects on the adsorption of methylene blue. 2016; 126:98–106.
- [22] Stawiński W, Węgrzyn A, Dańko T, et al. AC SC. ECSN. 2017; Available from: <http://dx.doi.org/10.1016/j.chemosphere.2017.01.039>.
- [23] Liu Y, Kang Y, Mu B, et al. Attapulgite / bentonite interactions for methylene blue adsorption characteristics from aqueous solution. *Chem. Eng. J.* [Internet]. 2014; 237:403–410. Available from: <http://dx.doi.org/10.1016/j.cej.2013.10.048>.
- [24] Elmoubarki R, Mahjoubi FZ, Tounsadi H, et al. Adsorption of textile dyes on raw and decanted Moroccan clays : Kinetics, equilibrium and thermodynamics. *Water Resour. Ind.* 2015; 9:16–29. Available from: <http://dx.doi.org/10.1016/j.wri.2014.11.001>.
- [25] Chinoune K, Bentaleb K, Bouberka Z, et al. Adsorption of reactive dyes from aqueous solution by dirty bentonite. *Appl. Clay Sci.* 2016; 123:64–75.
- [26] Vlasova, M, Dominguez-Patino G., Kakazey N., Mominguez-Patino M., Juarez-Romero D. EMY. Structural-Phase Transformations in Bentonite after Acid Treatment. *Sci. Sinter.* 2003; 35:155–166.
- [27] Hubicki Z., Zieba E. WG and RJ. FT-IR / PAS and SEM EDX Studies on Aluminosilicates Modified by Cs (I), Th (IV) and U (VI). *ACTA Phys. Pol. A.* 2009; 116:312–314.

- [28] Catrinescu C, Arsene D, Teodosiu C. Environmental Catalytic wet hydrogen peroxide oxidation of para -chlorophenol over Al / Fe pillared clays (AlFePILCs) prepared from different host clays. "Applied Catal. B, Environ. 2011; 101:451–460.
- [29] L. Cosmin Cotet, Andrada Măicăneanu CIF& VD. Alpha-Cypermethrin Pesticide Adsorption on Carbon Aerogel Aerogel and Xerogel. Sep. Sci. Technol. 2013; 37–41.
- [30] Ho Y-S. Citation review of Lagergren kinetic rate equation on adsorption reactions. Scientometrics. 2004; 59:171–177.
- [31] Ho YS, Llow GMFE. Kinetic Models for the Sorption of dye from Aqueous Solution by Wood. Trans IChemE. 1998; 76:183–191.
- [32] Kumar R, Rawat V, Banerjee S, et al. Synthesis of bimetallic Fe – Zn nanoparticles and its application towards adsorptive removal of carcinogenic dye malachite green and Congo red in water. J. Mol. Liq. 2015; 212:227–236.
- [33] Georgin J, Luiz G, Antonio M, et al. Preparation of activated carbon from peanut shell by conventional pyrolysis and microwave irradiation-pyrolysis to remove organic dyes from aqueous solutions. J. Environ. Chem. Eng. 2016; 4:266–275.
- [34] Lian L, Guo L, Wang A. Use of CaCl₂ modified bentonite for removal of Congo red dye from aqueous solutions. Desalin. 249. 2009; 249:797–801.
- [35] Langmuir I. The Adsorption of Gases on plane surface of Glass, Mica and Platinum. J. Am. Chem. Soc. 1918; 40:1361–1403.
- [36] Ali W, Hussain M, Ali M, et al. Evaluation of Freundlich and Langmuir Isotherm for Potassium Adsorption Phenomena. Int. J. Agric. Crop Sci. 2013; 6:1048–1054.
- [37] Ahmet, Çabuka, Tamer Akarb, Sibel Tunali b SG. Biosorption of Pb (II) by industrial strain of *Saccharomyces cerevisiae* immobilized on the biomatrix of cone biomass of *Pinus nigra* : Equilibrium and mechanism analysis. Chem. Eng. J. 2007; 131:293–300.
- [38] Reza M, Asfaram A, Hadipour A, et al. Kinetics and thermodynamic studies for removal of acid blue 129 from aqueous solution by almond shell. J. Environ. Heal. Sci. Eng. 2014; 1–7.
- [39] Dada, A.O, Olalekan, A.P, Olatunya, A.M., DADA O. Langmuir, Freundlich, Temkin and Dubinin – Radushkevich Isotherms Studies of Equilibrium Sorption of Zn²⁺ onto Phosphoric Acid Modified Rice Husk. IOSR J. Appl. Chem. 2012; 3:38–45.
- [40] Weber TW. Pore and Solid Diffusion Models for Fixed-Bed Adsorbers. AIChE J. 1974; 20:228–238.
- [41] Anayurt RA, Sari A, Tuzen M. Equilibrium , thermodynamic and kinetic studies on biosorption of Pb (II) and Cd (II) from aqueous solution by macrofungus (*Lactarius scrobiculatus*) biomass. Chem. Eng. J. 2009; 151:255–261.
- [42] Muthukumaran C, Murugaiyan V. Adsorption isotherms and kinetic studies of crystal violet dye removal from aqueous solution using surfactant modified magnetic nano-adsorbent. J. Taiwan Inst. Chem. Eng. 2016; 63:354–362.
- [43] Tosun İ. Ammonium Removal from Aqueous Solutions by Clinoptilolite : Determination of Isotherm and Thermodynamic Parameters and Comparison of

- Kinetics by the Double Exponential Model and Conventional Kinetic Models. *Int. J. Environ. Res. Public Health*. 2012; 9:970–984.
- [44] Singh M, Dosanjh HS, Singh H. Journal of Water Process Engineering Surface modified spinel cobalt ferrite nanoparticles for cationic dye removal : Kinetics and thermodynamics studies. *J. Water Process Eng.* [Internet]. 2016; 11:152–161. Available from: <http://dx.doi.org/10.1016/j.jwpe.2016.05.006>.
- [45] Wang W, Tian G, Wang D, et al. All-into-one strategy to synthesize mesoporous hybrid silicate microspheres from naturally rich red palygorskite clay as high- efficient adsorbents. *Nat. Publ. Gr.* 2016; 1–14. Available from: <http://dx.doi.org/10.1038/srep39599>.
- [46] Kannan C, Buvanewari N, Palvannan T. Removal of plant poisoning dyes by adsorption on Tomato Plant Root and green carbon from aqueous solution and its recovery. *DES.* 2009; 249:1132–1138. Available from: <http://dx.doi.org/10.1016/j.desal.2009.06.042>.
- [47] Eren E. Investigation of a basic dye removal from aqueous solution onto chemically modified Unye bentonite. *J. Hazard. Mater.* 2009; 166:88–93.
- [48] Anirudhan TS, Ramachandran M. Adsorptive removal of basic dyes from aqueous solutions by surfactant modified bentonite clay (organoclay): Kinetic and competitive adsorption isotherm. *Process Saf. Environ. Prot.* [Internet]. 2015; 95:215–225. Available from: <http://dx.doi.org/10.1016/j.psep.2015.03.003>.
- [49] Sharma V, Rekha P, Mohanty P. Nanoporous hypercrosslinked polyaniline : An efficient adsorbent for the adsorptive removal of cationic and anionic dyes. *J. Mol. Liq.* 2016; 222:1091–1100. Available from: <http://dx.doi.org/10.1016/j.molliq.2016.07.130>.
- [50] Makhoukhi B, Djab M, Didi MA. Journal of Environmental Chemical Engineering Adsorption of Telon dyes onto bis-imidazolium modified bentonite in aqueous solutions. *Biochem. Pharmacol.* [Internet]. 2015; 3:1384–1392. Available from: <http://dx.doi.org/10.1016/j.jece.2014.12.012>.



© 2018 by the author(s); licensee International Technology and Science Publications (ITS), this work for open access publication is under the Creative Commons Attribution International License (CC BY 4.0). (<http://creativecommons.org/licenses/by/4.0/>)